Journal of Applied Electrochemistry **29**: 939–949, 1999.

Niobium plating processes in alkali chloride melts

B. GILLESBERG[1], J.H. VON BARNER[1], N.J. BJERRUM[1]* and F. LANTELME[2]
[1]*Department of Chemistry, Technical University of Denmark, DK-2800 Lyngby, Denmark;*
[2]*Laboratoire d'Electrochimie, UMR 7612 CNRS, Université Pierre et Marie Curie, F-75252, Paris cedex 05, France (*author for correspondence)*

Received 21 July 1998; accepted in revised form 8 December 1998

Key words: electrodeposition, metal plating, molten salts, niobium, pulse electrolysis

Abstract

Niobium deposits were prepared from alkali chloride melts on nickel and AISI316 stainless steel substrates both by constant current and by pulse current methods. The influence of electrolysis conditions on the nature, morphology and purity of the deposits was investigated by X-ray diffraction, scanning electron microscopy and energy dispersive X-ray analysis. No metallic niobium was obtained at temperatures below 500 °C. At temperatures between 550 and 650 °C, the deposits were dendritic and non-adherent, whereas pure niobium layers could be obtained at 750 °C. Detailed analysis showed that a large negative overpotential during the pulse current period lead to the presence of suboxides, such as Nb_6O, in the metallic phase. Suitable electrolysis conditions gave pure oxygen-free niobium. Cross section analysis showed that on nickel a thin layer of niobium–nickel alloy such as $NbNi_3$, was formed at the metal interface. In contrast no alloys were detected at the niobium-stainless steel interface, where homogenous adherent layers of thickness around 50 μm were obtained.

1. Introduction

Electrodeposition of niobium has usually been carried out in fused alkali fluorides (esp. FLINAK) [1, 2]. Such melts are difficult to handle due to their toxic nature. The tendency is now to use alkali chlorides as solvents [3–5]. For example deposition of niobium from all chloride melts has been investigated by Rosenkilde and Østvold [6] who used the CsCl–NaCl eutectic and by Polyakov et al. [7] who used the CsCl–KCl–NaCl eutectic. However, CsCl is an expensive choice as solvent, and makes the process less interesting from an industrial point of view. Attempts to deposit niobium at low temperature, that is, around 200 °C, from chloroaluminate melts failed due to formation of insoluble subvalent niobium species [8]. $MgCl_2$–NaCl has also been a candidate as solvent for niobium salts, but, in this case, the reduction to metal showed a complicated behaviour which made the metal deposition less successful [9]. A solvent which has been applied in many connections is LiCl–KCl. Kuznetsov et al. [10] have shown that Nb^{4+} was reduced at the cathode to Nb^{2+} which subsequently reacted to form polyatomic compounds sparingly soluble in the melt. This made it impossible to obtain niobium of reasonable quality.

From the above it seems that attempts to produce niobium coatings from chloride melts have mostly been carried out at rather low temperatures, for example around 450 °C [3]. The scope of the present work is to investigate whether it is possible to plate high quality niobium layers from chloride melts at higher temperature than applied previously. Further, we investigate the influence of pulse plating conditions. We decided to apply low cost melts such as NaCl–KCl or LiCl–KCl as candidates for the solvent bath.

2. Experimental details

2.1. *Chemicals and apparatus*

The baths were prepared from pro analysis reagents (Merck). The LiCl–KCl (eutectic) or NaCl–KCl (equimolar) mixtures were purified according to a procedure involving carefully high vacuum desiccation and preelectrolysis. The salts were placed in the cell, which was evacuated ($p < 0.1$ mbar) for 24 h while the tempera-

ture was increased to approx. 150 °C below the melting point. Further heating was performed in dry argon atmosphere. After the salts were melted, the mixture was preelectrolysed (30 mA) for 8 h. The cell design resulted from a comparison between the constraints due to the aggressiveness of the melt and the need for easy handling of the electrodes and electrolyte. The apparatus for this study comprised a Hastelloy cell body and a glassy carbon crucible. This was covered by a glass cell lid with tight compression fittings (Torion) for tubing and electrode passage. The components of the apparatus were selected to achieve a vacuum tight cell at high temperature. The electrolysis experiments were performed under a dry argon atmosphere. The cell was placed in a general purpose electrical furnace.

To avoid evaporation of niobium species in the high oxidation states, for example, $NbCl_5$, the niobium was generated in oxidation state 3+. $NbCl_3$ was formed from niobium granules (Johnson Matthey) and anhydrous $NiCl_2$ according to the overall reaction $2\,Nb + 3\,Ni^{2+} \rightarrow 2\,Nb^{3+} + 3\,Ni$ [11]. $NiCl_2$ was prepared from $NiCl_2.6H_2O$ (Merck reagent), which was slowly heated under vacuum up to 150 °C, then a chlorine atmosphere was maintained up to 550 °C. The above reaction was confirmed by the determination of the niobium content of the bath by atomic absorption analysis. An excess of metallic niobium was used and the presence of a powdery layer of the alloy Ni_6Nb_7 at the surface of the niobium granules was characterised by X-ray diffraction (XRD). Thus, the reduction reaction can be written $11\,Nb + 6\,Ni^{2+} \rightarrow 4\,Nb^{3+} + Ni_6Nb_7$. No nickel was found in the molten salt solution, nor in the niobium deposit obtained on an inert electrode.

2.2. *Electrochemical conditions*

Nickel or AISI316 stainless steel plates (0.5 cm × 1 cm, thickness 0.5 mm) were used as cathodes for the deposition of niobium. For determination of the reaction mechanism the working electrode was made of a wire (1 mm dia.) of platinum or tungsten. The counter electrode was a sheet of pure niobium (3 cm × 2 cm, thickness 0.5 mm). As reference electrode a niobium wire was used. From measurements of the current involved in the oxidation of the platinum working electrode $\left(Pt \rightarrow Pt^{2+} + 2\,e^-\right)$ at different reverse potentials the equilibrium potential of the niobium reference electrode as $E^{\circ}_{Pt^{2+}/Pt}$ was found according to a procedure previously described [12]. Knowing the potential difference between $E^{\circ}_{Pt^{2+}/Pt}$ and the Ni^{2+}/Ni reference potentials makes it possible to relate potentials of the voltammetric measurements to the latter reference. The generation of the different potential or current programs was carried out with a Tacussel GSTP4 programmer. The transient responses were recorded on a Sefram X/Y recorder or stored temporarily in a Nicolet 310 digital oscilloscope.

2.3. *Applied plating programs*

Four types of plating program (A, B, C_1 and C_2) were applied. When pulse programs were applied, these were used in the most basic form, i.e. consisting of only two repeated current periods. The programs were chosen to cover a wide range concerning the average current density. High average current density favours short deposition times. On the other hand too high current densities will lead to deposits of poor quality. Average current densities up to above 100 mA cm^{-2} were applied for each plating program.

2.3.1. *Constant current (type A)*

Typically the current densities ranged between 22 and 222 mA cm^{-2}.

2.3.2. *Rest program (type B)*

The program consisted of repeated pulses (1 s) with intermediary rest periods (5 s) where no current passed. The aim of the rest period was to re-establish the equilibrium conditions in the melt. The current densities of the pulses, i_p, ranged from 177 to 694 mA cm^{-2} corresponding to average current densities between 30 and 116 mA cm^{-2}.

2.3.3. *Pulse peak programs (type C_1 and C_2)*

The programs consisted of short pulses of a high current superimposed on a constant basis current. The function of the superimposed signals was to initiate formation of new nuclei on the cathode and thereby discriminate formation of dendrites. The C_1 programs had a pulse period of 10 ms followed by a 1 s base period (i.e. with constant current). The current density during the pulses, i_p, ranged from 354 to 819 mA cm^{-2}. The base current density, i_b, was in the range from 20 to 170 mA cm^{-2}. In the C_2 programs the peak pulse period was 3 ms (i_p between 451 and 1029 mA cm^{-2}) and the base period 100 ms (i_b between 48 and 167 mA cm^{-2}). Due to the short duration of the pulses the average current densities were close to i_b for both the C_1 and C_2 programs.

3. Results and discussion

3.1. *Cyclic voltammetry*

Prior to the deposition experiments the melt was analysed by cyclic voltammetry. The results of such

experiments with different cathodic reverse potentials for the NaCl–KCl solvent are shown in Figure 1, which shows cyclic voltammograms recorded after several cycles. It can be seen that two reduction peaks, R_1 and R_2, appear at 0.1 and −0.4 V vs Ni^{2+}/Ni, respectively. They are coupled with two oxidation peaks Ox_1 at 0.35 V and Ox_2 at 0.1 V. The rest potential of the melt was measured as −0.1 V.

The NaCl–KCl–Nb(III) system has previously been studied in detail at a lower niobium concentration [11] from which it appears that Ox_1/R_1 is caused by the reversible redox process:

$$Nb^{4+} + e^- \leftrightarrow Nb^{3+} \quad (1)$$

The redox pair Ox_2/R_2 corresponds to the deposition and dissolution of the niobium metal according to

$$Nb^{3+} + 3e^- \leftrightarrow Nb \quad (2)$$

Since the value of the rest potential is between R_1 and R_2 the average valence of the melt was +3, confirming the results of the atomic absorption analysis (Section 2.1).

3.2. *Experiments in LiCl–KCl eutectic*

3.2.1. *450–550 °C*

In this temperature range it was not possible to produce coherent layers. Average current densities between 50 and 75 mA cm^{-2} were applied by both constant current and rest programs (type A and B, respectively). All the deposits were powdery and the metal substrate was poorly covered. The amount of material was too small for identification with XRD.

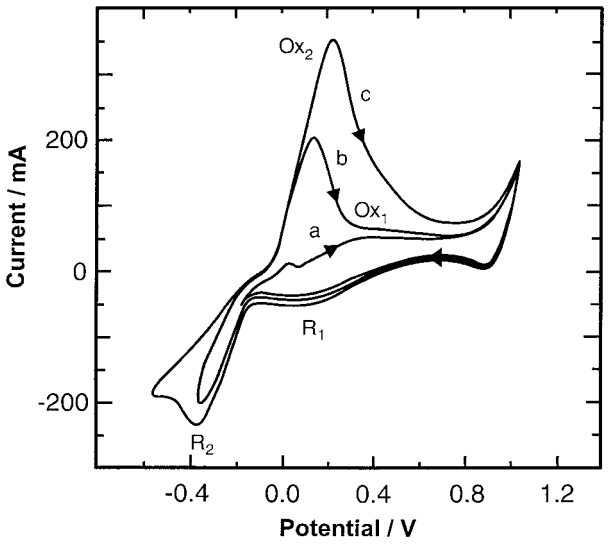

Fig. 1. Cyclic voltammogram at 750 °C in a NaCl–KCl equimolar melt containing 0.52 mol dm^{-3} Nb(III). Scan rate: 0.7 V s^{-1}. Working electrode: Pt (0.31 cm^2). Reference: Ni(II)(0.060 mol dm^{-3})/Ni.

3.2.2. *600 °C*

Thirteen experiments were performed with various average current densities by rest and pulse peak programs (type C_1). A survey of the experiments is shown in Figure 2. From this it appears that niobium, together with nickel alloys, was only obtained at high pulse current densities, at least 400 mA cm^{-2} was needed. At low current densities only signals from $NbNi_3$ and Ni were obtained on the XRD pattern of the surfaces. Raising the pulse current density made the amount of $NbNi_3$ less. For the deposits marked (1) and (2) in Figure 2 $(i_p = \sim 450\,\text{mA cm}^{-2})$ only the diffraction lines from niobium and the nickel substrate were detected. The deposit produced with the highest pulse current density (713 mA cm^{-2}, marked (3) in Figure 2) contained the largest amount of metallic niobium. This sample was investigated by scanning electron microscopy (SEM) and energy dispersive X-ray analysis (EDX). SEM pictures of the cross section and surface are shown in Figure 3. The deposited layer was porous and contained many cracks. From Figure 3(a) it appears that the thickness is unequal, ranging from 1 to 10 μm. Further, small bright inclusions can be seen. The EDX

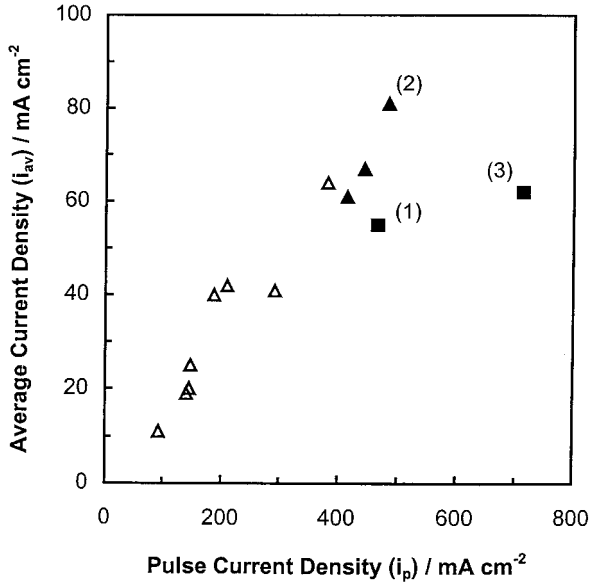

Fig. 2. Results of electrodepositions on nickel plates at 600 °C from LiCl–KCl eutectic melts as a function of the pulse current density, i_p, and average current density, i_{av}. Concentration of niobium ions, $c_{Nb(III)}$: 0.51 mol dm^{-3}. Applied deposition programs: (▲/△) Rest program (type B). (□/■) Pulse peak program (type C_1). Unfilled mark: no metallic niobium detected. Filled mark: the deposit contains metallic niobium.

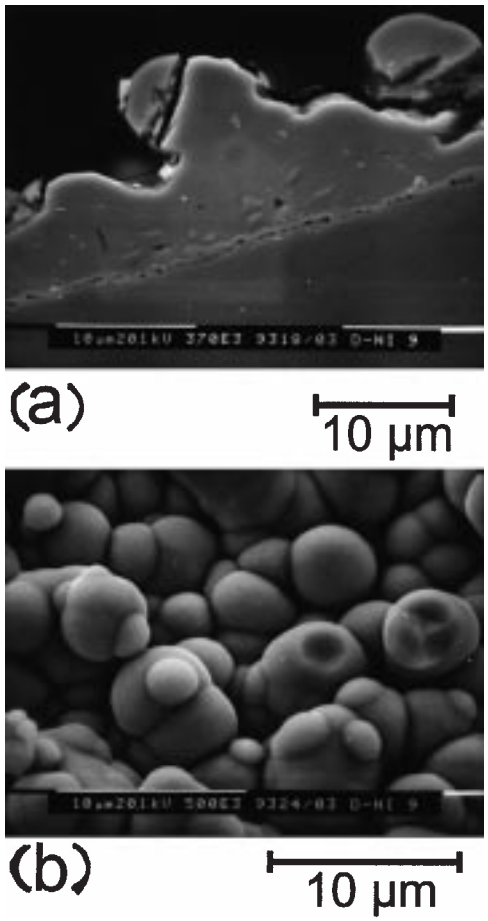

Fig. 3. SEM micrographs of the cross section (a) and the surface (b) of a niobium deposit from a LiCl–KCl eutectic melt at 600 °C on a nickel plate. Concentration of niobium ions, $c_{Nb(III)}$: 0.51 mol dm^{-3}. Pulse peak program (type C_1): $i_p = 713$ mA cm^{-2}; $i_b = 55$ mA cm^{-2}.

analysis of the bulk of the deposit gave: 90 at. % niobium, 7 at. % chlorine and 3 at. % nickel. A similar analysis of the inclusions only showed signals for niobium (46 at. %) and nickel (54 at. %). A transition layer with a thickness of about 0.5 μm was formed between the deposit and the substrate. This was, however, too thin to be analysed by EDX.

Thus, the results of XRD and EDX analysis are in good agreement, indicating the presence of elementary niobium and a nickel–niobium alloy with a high nickel content, probably $NbNi_3$. The presence of chloride may be due to the formation of subvalent niobium chlorides as was previously observed [3, 10].

3.2.3. *650 °C*

Eight experiments were performed with all three types of plating programs (A, B and C_1). At high average current densities (100 mA cm^{-2}) all the deposits contained niobium. At lower current densities niobium was occasionally found in the deposits. In general the coatings appeared to be more coherent than at 600 °C. The deposited layers were, however, still rather thin, approximately 5–15 μm.

3.2.4. *750 °C*

All the deposits, no matter what sort of plating programs were applied, contained niobium. Table 1 shows a survey of the XRD data of the sample surfaces. The deposits made with constant current or rest programs show only lines from metallic niobium. The deposit made with the peak pulse program (type C_1) shows some weak intensity diffraction lines besides the ones from metallic niobium. It is known that niobium forms solid solutions with oxygen up to approximately 1 at. % oxygen. For higher oxygen content between 13 and 18 at. % oxygen, Brauer et al. [13] have observed that lines in the XRD pattern are displaced somewhat compared to the pure metal. They suggested that a new phase with an approximate ratio Nb/O of 6 is formed. Compared to the strongest line of pure niobium metal with ($h\,k\,l = 1\,1\,0$) at $2\theta = 38.5°$, the strongest diffraction line of the 'Nb_6O' phase ($h\,k\,l = 1\,0\,1$) is positioned at a 2θ-angle equal to 38.3°. The weak lines in our XRD pattern for the type C_1 deposit (Table 1) are similar to the ones of 'Nb_6O', indicating that oxide is present in the deposit (content > 1 at. %).

Figure 4 shows SEM photographs of the cross section and the surface of a typical deposit made at 750 °C. The thickness of the deposited layer was considerably greater than before, approximately 50 μm (Figure 4(a)), and more homogenous than it was observed at lower temperatures. A few inclusions can be seen. An EDX analysis showed, that the bulk of the deposit contained more than 99 at. % pure niobium. Potassium (19 at. %) was detected in the inclusions besides niobium. The morphology of the surface can be seen in Figure 4(b) and 4(c). With the smaller magnification (Figure 4(b)), nodules of the same kind as observed in deposits from Flinak [1] melts are seen. The nodules and the rest of the surface are covered by crystals as can be seen clearly with greater magnification (Figure 4(c)). The crystals form a more coherent surface than at lower temperatures (see Figure 3(b)). Potassium containing impurities has also been observed in platings from FLINAK melts, but only when relatively large amounts of oxide (molar ratio O/Nb greater than one) was added [1].

3.3. *Experiments in equimolar NaCl–KCl*

Most of the plating experiments were performed in equimolar NaCl–KCl melt comprising a total of 45

Table 1. 2θ-values and intensities for XRD patterns of deposits on nickel substrates obtained from LiCl–KCl eutectic melts at 750 °C with different plating programs

Applied plating program						Literature data [13, 14]			
Type A i = 59 mA cm^{-2}		Type B i_p = 474 mA cm^{-2}		Type C_1 i_p = 676 mA cm^{-2} i_b = 97 mA cm^{-2}		Species	2θ /°	$h\,k\,l$	Rel. int. /%
2θ /°	Intensity /CPS	2θ /°	Intensity /CPS	2θ /°	Intensity /CPS				
				38.2	39	Nb_6O	38.269	1 0 1	100
38.6	396	38.6	392	38.5	480	Nb	38.475	1 1 0	100
55.7	120	55.5	38	55.5	68	Nb	55.542	2 0 0	16
69.7	572	69.7	749	69.2	512	Nb	69.587	2 1 1	20
82.4	76	82.5	43	82.2	80	Nb	82.454	2 2 0	5
94.9	72	94.9	56	94.7	104	Nb	94.903	3 1 0	4
				~106	152	Nb_6O	105.611	2 2 2	40
107.5	240	107.6	131	~106	132	Nb	107.602	2 2 2	1
				~120	164	Nb_6O	120.781	2 1 3	60
121.1	180	121.2	123	~120	168	Nb	121.286	3 2 1	4

different types. Because of the relatively high melting point of the solvent (685 °C) we chose to apply a temperature of 750 °C for all experiments.

3.3.1. *Constant current electrolysis (type A)*
The current density was varied in the region 22 to 220 mA cm^{-2}. Nodules were observed on all of the deposits (e.g., Figure 5(a)), but polycrystalline regions (Figure 5(b) and (c)) constituted the greatest part of the surfaces.

The XRD patterns (Figure 6) showed signals from niobium, but the intensities were different from what has normally been seen. Especially the diffraction from the $h\,k\,l = 2\,1\,1$ plane were stronger than usual. This effect seems to be even more pronounced at the highest (220 mA cm^{-2}) current density. It thus appears, that there is a preferred growth in the $h\,k\,l = 2\,1\,1$ direction of the deposit produced with a constant current. It can be noticed that the 2θ-value for the $h\,k\,l = 1\,1\,0$ diffraction is displaced towards slightly lower values with increasing current density (e.g., Table 2). This could point in the direction of the presence of oxygen in the deposit as mentioned for the deposit obtained with C_1-type program from LiCl–KCl melts at 750 °C (Table 1). Further it seems that the ($h\,k\,l = 2\,1\,1$) diffraction around $2\theta = 69°$, becomes rather broad as the current density increases. This may also indicate the presence of oxide since this peak, may be due to two peaks (one at 69.5° due to metallic niobium and the other at 68.2° due to Nb_6O).

3.3.2. *'Rest' electrolysis (type B)*
Five experiments were performed with pulse current densities ranging from 185 to 694 mA cm^{-2}. The latter current density was obviously too high, since a nonmetallic black product was formed at the electrode surface. The layer showed poor adherence to the substrate.

At lower current densities layers with a thickness of 10–30 μm were produced (Figure 7). An EDX analysis showed that the bulk of these layers was pure niobium. It can be seen from Figure 7 that two layers, which differ from the bulk layer, are present at the interface between deposit and substrate. An EDX analysis of these transitions showed that the layer closest to the nickel substrate consisted of 74 at. % nickel and 26 at. % niobium. According to this analysis it seems very likely that the well known compound $NbNi_3$ (75 at. % Ni) is formed. A slightly lower nickel content was observed in the transition when a higher current density, 427 mA cm^{-2} was applied. In this case 68 at. % nickel and 32 at. % niobium were found.

The XRD pattern of the surface showed that the deposits were not pure niobium since the strongest diffraction line was at $2\theta = 38.3°$. We also found other diffraction lines due to the presence of oxygen in the metal, that is, the Nb_6O phase which has been discussed in previous paragraphs concerning LiCl–KCl melts. Further traces of nickel and of niobium–nickel alloys were also seen.

At the lowest pulse current density, 185 mA cm^{-2}, the surface was smooth (Figure 8(a)). When the current density was increased nodules of the same type as already observed in deposits from LiCl–KCl melts appeared (see Figure 4(b) and 4(c)). However, crystallites, like in Figure 8(b), covered the whole surface.

At a very high pulse current density, 694 mA cm^{-2}, a black and badly adherent surface layer was obtained.

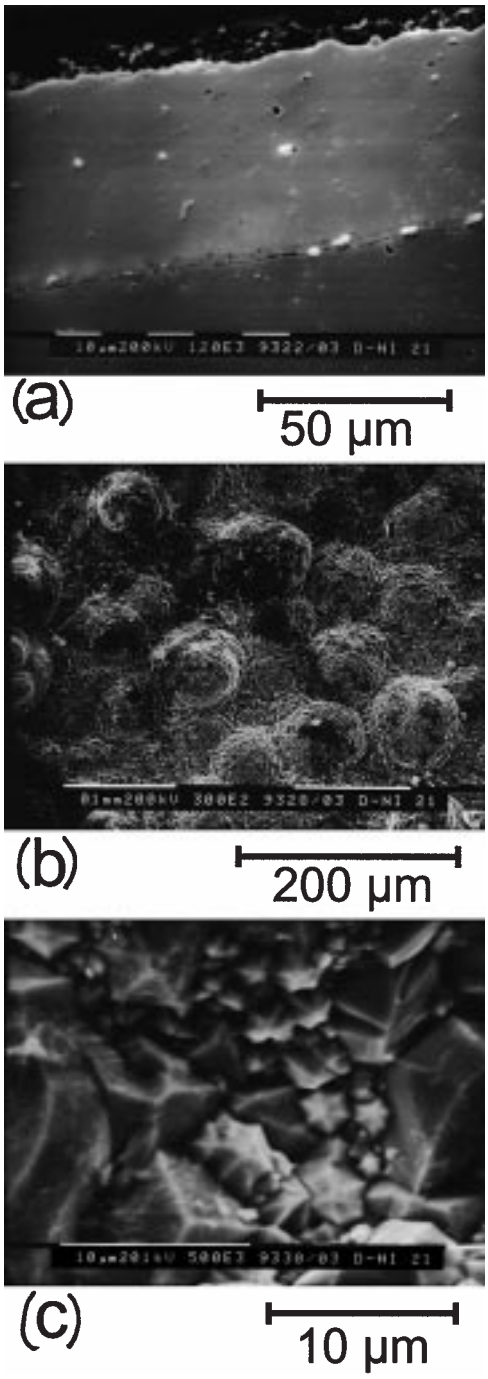

Fig. 4. SEM micrographs of the cross section (a) and the surface (b and c) of a niobium deposit on a nickel plate from a LiCl–KCl eutectic melt at 750 °C. Concentration of niobium ions, $c_{Nb(III)}$: 0.51 mol dm^{-3}. Pulse peak program (type C_1): $i_p = 676$ mA cm^{-2}; $i_b = 97$ mA cm^{-2}.

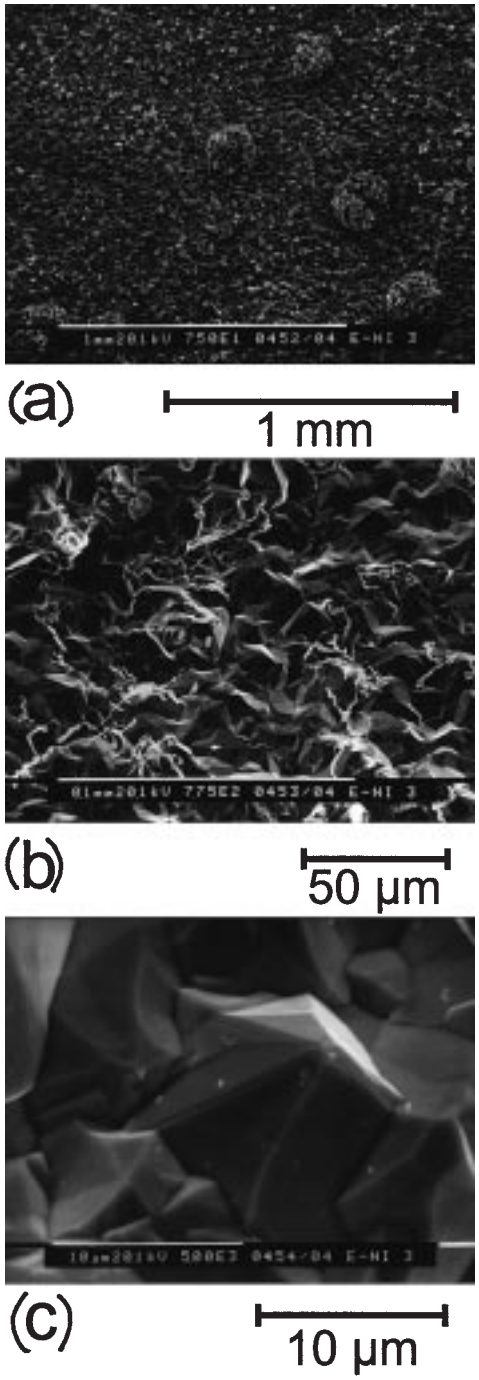

Fig. 5. SEM micrographs of the surface of niobium deposited on nickel from a NaCl–KCl equimolar melt at 750 °C. Concentration of niobium ions, $c_{Nb(III)}$: 0.49 mol dm^{-3}. Constant current electrolysis (type A): $i = 22$ mA cm^{-2}.

Unfortunately, it was impossible to identify the product by XRD. As can be seen from Figure 9, the cathodic potentials during the pulse period changed with time. Generally, the potentials became less negative with time and after 20 min they reached a plateau. The change was more pronounced at high pulse current densities. The

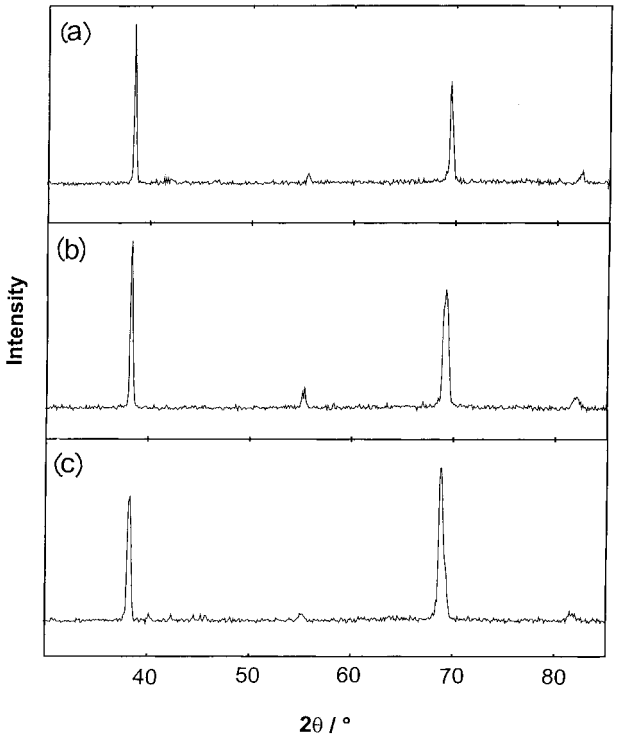

Fig. 6. X-ray diffraction patterns of electrodeposits obtained at 750 °C from a NaCl–KCl equimolar melt. Concentration of niobium ions, $c_{Nb(III)}$: 0.49 mol dm^{-3}. Constant current electrolysis (type A). Current densities, i : (a) 22, (b) 74 and (c) 220 mA cm^{-2}.

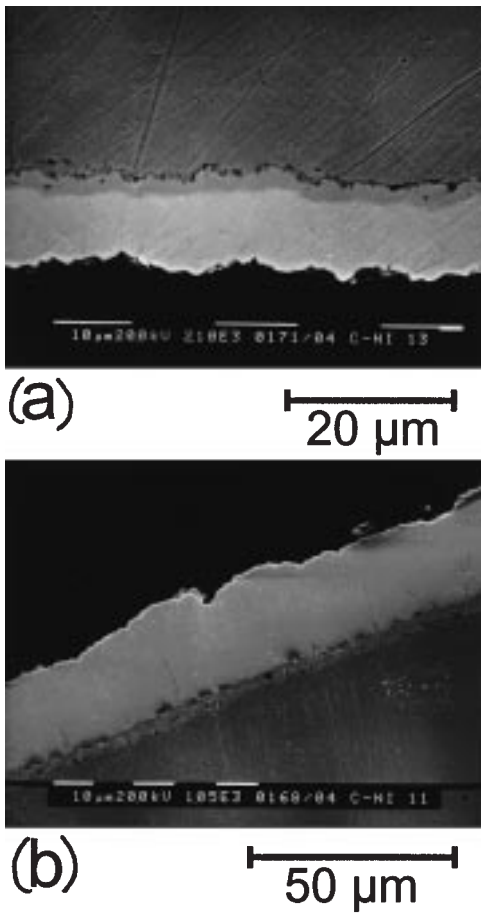

Fig. 7. SEM micrographs (cross sections) of niobium deposited on nickel from a NaCl–KCl equimolar melt at 750 °C. *Note*: (a) is here with surface down. Concentration of niobium ions, $c_{Nb(III)}$: 0.52 mol dm^{-3}. Rest programs (type B). Pulse current densities (i_p): (a) 185 and (b) 350 mA cm^{-2}.

more negative potential values for high current density may explain why the deposit became heterogeneous and not satisfactory from an applied point of view. A similar behaviour has been observed before for layers of other refractory metals such as tantalum, where a high negative deposition potential gave rise to nonmetallic deposits [15].

3.3.3. *Pulse peak electrolysis (type C_1)*

Both the pulse current density and the base current density were varied during these experiments. The pulses (10 ms) had a current density, i_P, between 354 and 819 mA cm^{-2}, while the base current density, i_b, were given values between 20 and 170 mA cm^{-2}. Table 3 shows a comparison between the primary diffraction values of deposits produced with equal pulse current density, i_p, but with a variation of the base current density, i_b, from 22 to 85 mA cm^{-2}. For all the deposits the strongest diffractions were at 2θ-values near 38° and

Table 2. Characteristics of the XRD patterns shown in Figure 6 compared to literature data

Figure 6(a)		Figure 6(b)		Figure 6(c)		Literature Data [14]			
2θ /°	Intensity /CPS	2θ /°	Intensity /CPS	2θ /°	Intensity /CPS	Species	2θ /°	*h k l*	Rel. int. /%
38.5	447	38.4	662	38.3	413	Nb	38.475	1 1 0	100
55.6	36	55.4	56	55.2	36	Nb	55.542	2 0 0	16
69.6	291	69.2	374	68.8	509	Nb	69.587	2 1 1	20
82.5	41	82.2	47	81.8	39	Nb	82.454	2 2 0	5

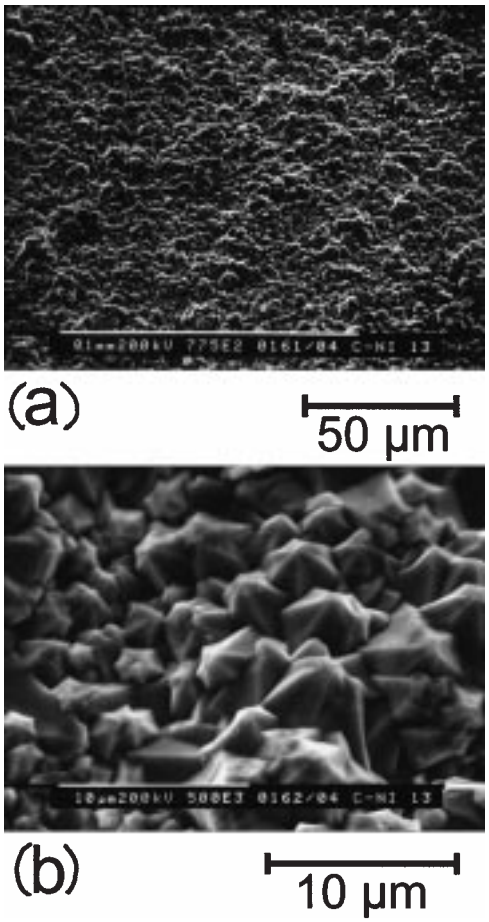

Fig. 8. SEM micrographs of the surface of niobium deposited from a NaCl–KCl equimolar melt at 750 °C. Concentration of niobium ions, $c_{Nb(III)}$: 0.52 mol dm^{-3}. Rest programs (type B). Pulse current densities, i_p: (a) 185 and (b) 350 mA cm^{-2}.

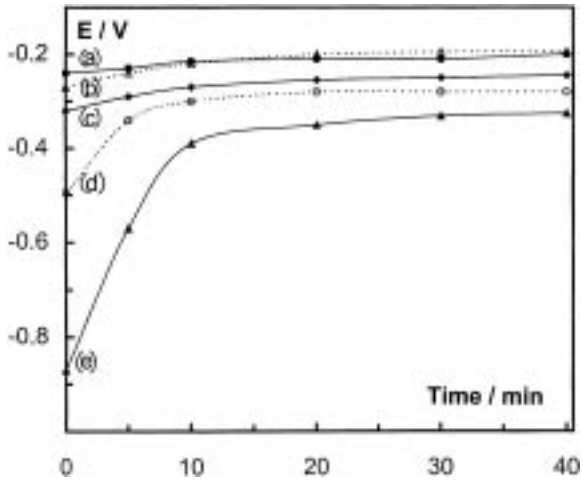

Fig. 9. Variation of the electrode potential during the electrolysis from a NaCl–KCl equimolar melt at 750 °C. Concentration of niobium ions, $c_{Nb(III)}$: 0.52 mol dm^{-3}. Substrate: nickel. Reference: Ni(II) (0.060 mol dm^{-3}) / Ni. Rest programs (type B). Pulse current densities, i_p: (a) 177, (b) 185, (c) 355, (d) 427 and (e) 694 mA cm^{-2}.

69°. Weaker signals were observed around 55° and 82°. The observed diffractions are compared with 2θ-values from the literature for niobium and the previously mentioned 'Nb_6O' phase [13].

It can be seen from Table 3 that the deposit produced with the lowest current density shows signals from niobium metal only. When the current density is increased, a weak displacement towards lower 2θ-values occurs. This effect is clearly visible in Figure 10, which shows a magnified section of XRD pattern in the 2θ region 37–39°. If we further take into account the other 2θ-values reported in Table 3, it seems that an increase of the overall current density produces more oxygen in the deposit, as also observed for deposits produced with

Table 3. Characteristics of the XRD patterns of electrodeposits obtained form a NaCl–KCl equimolar melt at 750 °C using pulse peak programs (type C_1) with constant pulse current density (i_p = 550 mA cm^{-2}) and varying basis current density. Concentration of niobium ions, $c_{Nb(III)}$: 0.49 mol dm^{-3}. Observed signals are compared to data from the literature

i_b = 22 mA cm^{-2}		i_b = 77 mA cm^{-2}		i_b = 85 mA cm^{-2}		Literature data [13,14]			
2θ /°	Int. /CPS	2θ /°	Int. /CPS	2θ /°	Int. /CPS	Species	2θ /°	*h k l*	Rel. int. /%
		38.3	978	38.2	331	Nb_6O	38.269	1 0 1	100
38.5	210					Nb	38.475	1 1 0	100
		55.2	48	55.1	40	Nb_6O	54.129	2 0 0	40
55.7	142	55.2		55.1		Nb	55.542	2 0 0	16
		~68.9	475	~68.9	556	Nb_6O	68.198	2 1 1	70
		~68.9		~68.9		Nb_6O	69.465	1 1 2	50
69.7	269	~68.9		~68.9		Nb	69.587	2 1 1	20
		81.9	87	81.8	42	Nb_6O	81.842	2 0 2	40
82.5	52					Nb	82.454	2 2 0	5

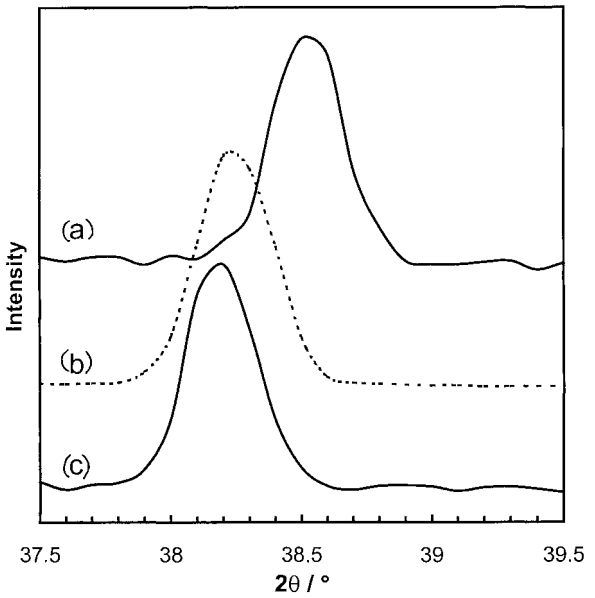

Fig. 10. Magnified section of the X-ray diffraction patterns in the 2θ region 37–39° of deposits obtained at 750 °C from a NaCl–KCl equimolar melt containing Nb(III) (0.49 mol dm^{-3}) with pulse peak program type C_1. Pulse current density (i_p): 550 mA cm^{-2}. Basis current densities, i_b: (a) 22, (b) 77 and (c) 85 mA cm^{-2}.

the rest programs (type B). This trend is in good agreement with our previous work which showed that a high negative overpotential enhanced the oxygen activity in the metallic niobium when oxide ions were present in the electrolyte [5].

Figure 11 shows a SEM photograph of the deposit produced with a base current density of 77 mA cm^{-2}. It should be noticed that no nodules appear at the surface. The crystallites have a size of approximately 5 μm and form a coherent surface layer. Changes in the base current density, i_b, in the range from 22 to 85 mA cm^{-2} had only a small influence on the morphology of the surface seen in Figure 11, except for some minor changes in the grain size.

Since we have just seen that a low overall current density seems to favour the absence of oxygen in the layer produced, it was decided to investigate the influence of the pulse current density, i_p, in experiments with low base current density $(i_b \approx 30\ \text{mA cm}^{-2})$. The pulse current density, i_p, was varied from 368 to 708 mA cm^{-2}. All the XRD patterns showed the four strongest reflections for oxygen-free niobium metal; no other lines were observed. It was further noticed that the crystals have a preferred orientation in the $h\,k\,l = 2\,1\,1$ direction. This effect was more pronounced with higher pulse current densities.

The surfaces of the crystals changed considerably with the pulse current density. At a low value, i_p = 368 mA cm^{-2}, a relatively large variation (1–20 μm) in the crystal size was observed as shown in Figure 12. Further, several dendrites were present in this deposit. Raising the pulse current implies that no dendrites appear (Figure 13). Moreover the grain size variation was small, most of the grains were in the range from 2 to 5 μm. The deposit performed with a pulse current of 708 mA cm^{-2} were rather similar to the one shown in Figure 13.

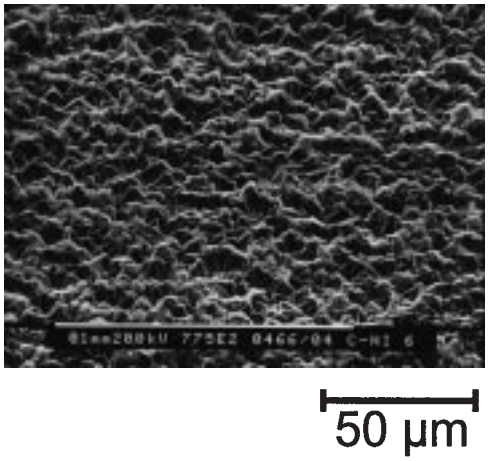

Fig. 11. SEM micrograph of the surface of a niobium deposit on nickel from a NaCl–KCl equimolar melt at 750 °C. Pulse peak program (type C_1): $i_p = 550$ mA cm^{-2}; $i_b = 77$ mA cm^{-2}.

3.3.4. *Pulse peak electrolysis (type C_2)*

A shorter duration of the pulse period (3 ms) and of the base current (100 ms), i.e. type C_2 programs, seemed to have no beneficial effect. A variation of the pulse current

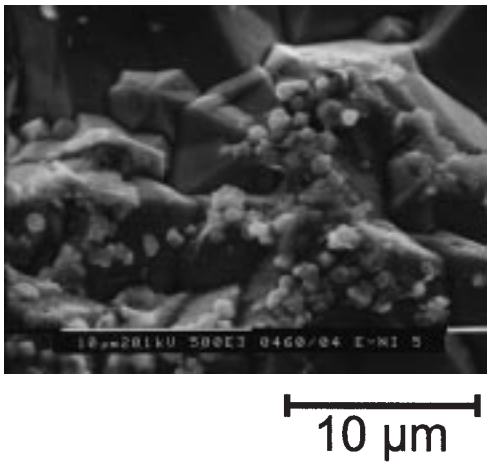

Fig. 12. SEM micrograph of the surface of a niobium deposit performed on a nickel plate from a NaCl–KCl equimolar melt at 750 °C. Concentration of niobium ions, $c_{Nb(III)}$: 0.50 mol dm^{-3}. Pulse peak program (type C_1): $i_p = 368$ mA cm^{-2}; $i_b = 36$ mA cm^{-2}.

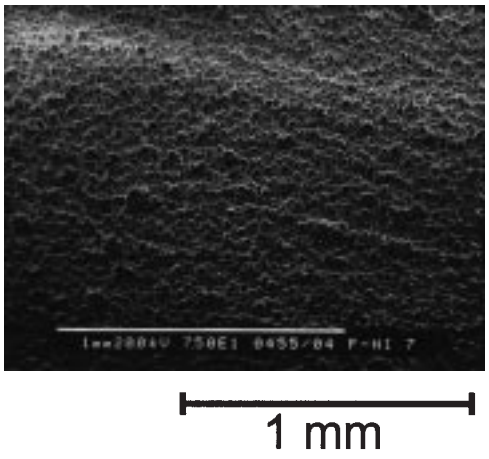

Fig. 13. SEM micrograph of the surface of a niobium deposit performed on a nickel plate from a NaCl–KCl equimolar melt at 750 °C. Concentration of niobium ions, $c_{Nb(III)}$: 0.50 mol dm^{-3}. Pulse peak program (type C_1): $i_p = 511\,mA\,cm^{-2}$; $i_b = 30\,mA\,cm^{-2}$.

density, i_p, between 450 and 708 mA cm^{-2} with a base current, i_b, of approximately 20 mA cm^{-2}, gave deposits of a reasonable quality.

3.3.5. *Experiment on stainless steel*

Pulse plating experiments were also performed on an AISI316 stainless steel substrate. For a deposit produced with a pulse current density, $i_p = 622\,mA\,cm^{-2}$, and a base current density, $i_b = 23\,mA\,cm^{-2}$ (type C_1 program), the XRD pattern showed the four strongest lines of niobium metal with a preferred orientation in the $h\,k\,l = 2\,1\,1$ direction. SEM photographs of the cross section and surface of the deposit are shown in Figure 14. It clearly appears that there is no transition layer between the substrate and the deposit (Figure 14(a)). The plated layer is very uniform with a thickness of approximately 60 μm, and no inclusions are seen in the bulk of the layer. An EDX analysis showed only signals due to pure niobium metal. The surface consisted of small crystals with an almost uniform size of 7 μm. The layer was very coherent and the adherence to the substrate was excellent.

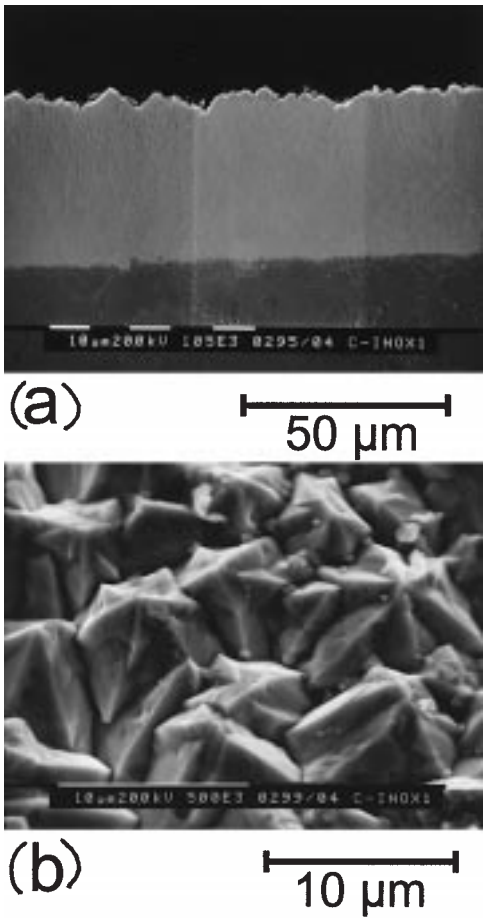

Fig. 14. SEM micrographs of the cross section (a) and the surface (b) of a niobium deposit performed on a stainless steel (AISI316) plate from a NaCl–KCl equimolar melt at 750 °C. Concentration of niobium ions, $c_{Nb(III)}$: 0.50 mol dm^{-3}. Pulse peak program (type C_1): $i_p = 622\,mA\,cm^{-2}$; $i_b = 23\,mA\,cm^{-2}$.

4. Conclusion

The present work shows the strong influence of temperature on niobium plating. This influence was demonstrated using the eutectic mixture LiCl–KCl as solvent. At low temperatures (i.e., below $\sim$ 550 °C) no coherent layers were obtained. At temperatures between 550 and 650 °C niobium layers were obtained; however, they remained heterogeneous and contained many inclusions. At 750 °C homogeneous layers of metallic niobium were deposited from both LiCl–KCl and NaCl–KCl melts. It has previously been shown that coherent niobium layers of poor quality can be obtained from equimolar mixture NaCl–KCl melts at the latter temperature. Experiments carried out at lower temperatures in LiCl–KCl were even less satisfactory. It was concluded that LiCl–KCl is an inconvenient electrolyte for performing niobium deposition. In fact, this does not seem to be the case, since our work shows that the quality of the deposits are very much the same whether LiCl–KCl or NaCl–KCl are used as solvent at 750 °C.

Another conclusion is that all chloride electrolytes can be used to produce high quality niobium deposits. Following the initial work of Mellors and Senderoff [16], it was assumed that alkali fluorides were the best electrolytes for niobium plating. In FLINAK, Christensen et al. [1] have shown that at low temperatures (below

600 °C) no coherent niobium deposits are obtained. As in alkali chloride melts a temperature of at least 700 °C is required to form high quality coatings. In fluoride melts the presence of oxide ions may have a beneficial effect concerning the electrochemical reduction and the Faraday yield. All chloride melts seems to be more sensitive, since traces of oxides in the melts may lead to the presence of oxygen in the metallic deposit. This is certainly due to the positive shift in the potential of the suboxide formation when no fluoride ions are present in the solution [5]. However, this consequence can be overcome by choosing suitable electrolysis conditions avoiding too negative overpotentials.

Acknowledgements

We gratefully acknowledge the financial support from the Human Capital and Mobility Programme of the EEC in the frame of the project 'Physical Chemistry of Metal-Molten Salt Solutions in the Production of Light and Refractory Metals'.

References

1. E. Christensen, X. Wang, J.H. von Barner, T. Østvold and N.J. Bjerrum, *J. Electrochem. Soc.* **141** (1994) 1212.
2. P. Chamelot, B. Lafage and P. Taxil, *Electrochim. Acta* **43** (1997) 607.
3. F. Lantelme, A. Barhoun and J. Chevalet, *J. Electrochem. Soc.* **140** (1993) 324.
4. L. Arurault, J. Bouteillon and J.C. Poignet, *J. Electrochem . Soc.* **142** (1995) 3351.
5. F. Lantelme, Y. Berghoute, J.H. von Barner and G.S. Picard, *J. Electrochem. Soc.* **142** (1995) 4097.
6. C. Rosenkilde and T. Østvold, *Acta Chem. Scan.* **49** (1995) 85.
7. I.R. Elizarova, E.G. Polyakov and L.P. Polyakova, *Soviet Electrochem.* **27** (1991) 581.
8. K.D. Sienerth, E.M. Hondrogiannis and G. Mamantov, *J. Electrochem. Soc.* **141** (1994) 1762.
9. M. Mohamedi, N. Kawaguchi, Y. Sato and T. Yamamura, **PV 96–7**, *The Electrochemical Society Proceedings Series*, Pennington, NJ, p. 189. (1996).
10. S.A. Kuznetsov, A.G. Morachevskii and P.T. Stangrit, *Soviet Electrochem.* **18** (1982) 1357.
11. F. Lantelme and Y. Berghoute, *J. Electrochem. Soc.* **141** (1994) 3306.
12. Y. Berghoute, A. Salmi and F. Lantelme, *J. Electroanal. Chem.* **365** (1994) 171.
13. G. Brauer, H. Müller and G. Kühner, *J. Less-Comm. Metals* **4** (1962) 533.
14. US National Bureau of Standards, *Monogr.* ***25*** **19** (1982) 67.
15. F. Lantelme, A. Barhoun, G. Li and J-P. Besse, *J. Electrochem. Soc.* **139** (1992) 1259.
16. G.W. Mellors and S. Senderoff, *J. Electrochem. Soc.* **112** (1965) 266.